Published for SISSA by Springer

Received: *January 25, 2011*
Accepted: *February 11, 2011*
Published: *February 25, 2011*

JHEP02(2011)105

The sphaleron rate in SU(N) gauge theory

Guy D. Moore and Marcus Tassler

Department of Physics, McGill University,
3600 rue University, Montréal, QC H3A 2T8, Canada

E-mail: guymoore@physics.mcgill.ca, tassler@hep.physics.mcgill.ca

Abstract: The sphaleron rate is defined as the diffusion constant for topological number $N_{\rm CS} \equiv \int \frac{g^2 F\tilde{F}}{32\pi^2}$. It establishes the rate of equilibration of axial light quark number in QCD and is of interest both in electroweak baryogenesis and possibly in heavy ion collisions. We calculate the weak-coupling behavior of the SU(3) sphaleron rate, as well as making the most sensible extrapolation towards intermediate coupling which we can. We also study the behavior of the sphaleron rate at weak coupling at large $N_{\rm c}$.

Keywords: Thermal Field Theory, Lattice Gauge Field Theories, Solitons Monopoles and Instantons, QCD

ArXiv ePrint: 1011.1167

doi:10.1007/JHEP02(2011)105

Contents

JHEP02(2011)105

1 Introduction

It has long been known [1] that Yang-Mills theory possesses multiple classical vacua, distinguished by a topological number, the Chern-Simons number. No continuous sequence of infinitesimal gauge transformations can bring one of these vacua into another; instead a "large" gauge transformation of nontrivial topology is needed. The topological character of the gauge transformations is ensured by the nontrivial homotopy of the gauge group, e.g. $\pi_3(G) = \mathcal{Z}$ for $G = \mathrm{SU}(N_{\rm c})$, $N_{\rm c} \geq 2$.

This topological nature of the vacuum has important physical consequences because of the chiral (ABJ) anomaly [2, 3]. The would-be conserved current associated with a left-handed fermion in the fundamental representation is[1]

$$\partial_\mu J^\mu_{\rm L}(X) = \frac{g^2}{32\pi^2} F^a_{\mu\nu} \tilde{F}^{\mu\nu}_a(X)\,, \qquad \tilde{F}^{\mu\nu} \equiv \frac{1}{2}\epsilon^{\mu\nu\alpha\beta} F_{\alpha\beta}\,. \tag{1.1}$$

Within the Standard Model, this has a few very interesting consequences. The $\mathrm{SU_L}(2)$ weak-hypercharge group couples only to left-handed fields, so the anomaly gives rise to baryon and lepton number violation [4]. While under ordinary conditions these have essentially no physical consequences, at very high temperatures where electroweak symmetry is "restored," baryon and lepton number violation becomes efficient [5–7], opening the possibility of electroweak baryogenesis [8, 9]. The $\mathrm{SU_C}(3)$ color group couples to equal numbers

[1] Our conventions are that $g_{\mu\nu} = \eta_{\mu\nu} = \mathrm{Diag}[-+++]$, and that capital letters X, P are 4-vectors with $t = x^0$, $\omega = p^0$ and $\boldsymbol{x}, \boldsymbol{p}$ are the 3-vector components. Lower case x, p are reserved to denote $|\boldsymbol{x}|, |\boldsymbol{p}|$.

of left and right handed fields[2] and so no global symmetry violation is associated with it. However, the up and down quark flavors are extremely light, so the anomaly is the most efficient way of interchanging left with right handed first generation quarks.

The equilibration of right- and left-handed quark number is important to baryogenesis, and therefore the strong sphaleron rate is too; see for instance [10–13]. The same applies to heavy ion collisions, which also appear to involve the production of a hot quark-gluon plasma [14–17]. Indeed, recently Kharzeev, McLerran and Warringa have argued that topological fluctuations may play an important role in *creating* local fluctuations or imbalances in left-handed versus right-handed quark number [18, 19], which could have very interesting experimental signatures [20, 21].

The relation between real (Minkowski) time topology change and Euclidean topological susceptibility is subtle (see [22] and the discussion below). Therefore the Minkowski rate of topology fluctuation cannot be easily inferred from Euclidean quantities and needs to be separately studied. There is a vast literature on doing so for the $\mathrm{SU_L}(2)$ sector of the Standard Model [6, 7, 23–35], and it would be fair to say that the efficiency of topology change is well understood for this group and at the relevant coupling. But $\mathrm{SU_C}(3)$ has been much less carefully studied. At this time, there are two quite different parametric estimates [10, 36], as well as a rather crude calculation [37] which was made before our modern understanding of the parametric behavior was developed [30, 31]. Therefore, particularly in the light of the recent resurgence of interest in topology change in the strong interactions [18, 19], we think it is timely to revisit the question of the "strong sphaleron rate," the (equilibrium, thermal) rate of topology change in the group SU(3). As we will discuss momentarily, we currently only know of tools to do so at weak coupling, so we will be forced to restrict our attention to weak coupling. However we will also make the most reasonable estimate we can of the rate at intermediate coupling.

For the impatient reader, we summarize our results here: the rate of topology change per spacetime volume is defined as

$$\Gamma_{\mathrm{sphal}} \equiv \lim_{t\to\infty} \frac{(N_{\mathrm{CS}}(t) - N_{\mathrm{CS}}(0))^2}{Vt} = \int d^4X \left\langle \frac{g^2}{32\pi^2} F^a_{\mu\nu}\tilde{F}^{\mu\nu}_a(X)\, \frac{g^2}{32\pi^2} F^a_{\alpha\beta}\tilde{F}^{\alpha\beta}_a(0) \right\rangle \tag{1.2}$$

where the $t \to \infty$ (zero frequency) limit is to be taken with some care, see below. In the limit of high temperature (and hence of weak coupling), the temperature and coupling dependence for $\mathrm{SU}(N_{\mathrm{c}}{=}3)$ is ($\alpha_{\mathrm{s}} = g^2/4\pi$)

$$\Gamma_{\mathrm{sphal}} = (132 \pm 4) \left(\frac{g^2T^2}{m_{\mathrm{D}}^2}\right) \left(\ln\frac{m_{\mathrm{D}}}{\gamma} + 3.0410\right) \alpha_{\mathrm{s}}^5 T^4 \,, \tag{1.3}$$

$$\gamma = \frac{N_{\mathrm{c}} g^2 T}{4\pi} \left(\ln\frac{m_{\mathrm{D}}}{\gamma} + 3.041\right) \,, \tag{1.4}$$

$$m_{\mathrm{D}}^2 = \frac{2N_{\mathrm{c}} + N_{\mathrm{f}}}{6} g^2T^2 = \frac{6 + N_{\mathrm{f}}}{6} g^2T^2 \,. \tag{1.5}$$

Note that γ, the mean rate of color randomization, is defined self-referentially, and should be found self-consistently [34, 35].

[2] Or equivalently, to equal numbers of left-handed fields in the fundamental and antifundamental representations.

JHEP02(2011)105

The N_c scaling is surprisingly simple; investigating $N_c = 2, 3, 5, 8$ we find that

$$\Gamma_{\rm sphal} = (0.21 \pm 0.01) \left(\frac{N_c g^2 T}{m_D^2}\right) \left(\ln \frac{m_D}{\gamma} + 3.0410\right) \frac{N_c^2 - 1}{N_c^2} (N_c \alpha)^5 T^4 \tag{1.6}$$

with no further N_c corrections visible within our error bars. The functional form and even the numerical value are in good agreement with the conjecture of [36].

The formal range of validity of the above results is very narrow; not only the coupling α_s, but even the inverse log of the coupling $1/\ln(1/\alpha_s)$ must be small. At larger coupling we can *estimate* the sphaleron rate based on the diffusion rate of a lattice-regulated, classical field theory with the same magnetic-field damping rate as the leading-order result we find in the quantum theory. This approach is known to be correct in the weak coupling limit [30, 31, 38] but at larger coupling values it amounts to a crude estimate; the dynamics cease to be well described by classical field theory, and the classical lattice model sees more and more "lattice-y" dynamics artifacts. We can also only push the lattice to a certain level of coarseness before it becomes impossible to establish any topological character for the fields. As shown in table 3, this allows access to $\alpha_s \lesssim 0.1$. The leading-log results work reasonably well for $\alpha_s \lesssim 0.03$ but break down after this. And the classical framework starts to break down above about $\alpha_s = 0.1$.

The remainder of the paper is organized as follows. In section 2 we review the definition and utility of the sphaleron rate, its relation to Euclidean correlation functions, and the extreme difficulty of its determination from lattice Euclidean data. Then section 3 reviews the effective field theories valid at weak coupling and presents the details of our numerical implementation and calculation. Section 4 presents our numerical results for the weak-coupling sphaleron rate and section 5 presents the best extrapolation towards intermediate coupling we can achieve. We discuss applications in section 6.

2 Sphaleron rate: generalities

Here we review the definition and physical relevance of the sphaleron rate, and its relation to Euclidean correlation functions. Nothing in this section is new, it is included as a refresher for readers familiar with the issues and an introduction for readers who are not.

2.1 Definition of the sphaleron rate

As mentioned above, the axial current associated with a quark species,

$$J^\mu_{A,q} \equiv \bar{q} \gamma^\mu \gamma_5 q \tag{2.1}$$

is not conserved. There are actually two contributions to its nonconservation: the quark mass, which explicitly breaks the axial symmetry, and the chiral anomaly:[3]

$$\partial_\mu J^\mu_{A,q} = 2 m_q \bar{q} \gamma_5 q - 2 \frac{g^2}{32\pi^2} F^a_{\mu\nu} \tilde{F}^{\mu\nu}_a \tag{2.2}$$

[3] From now on we specialize to vectorlike theories with fundamental representation matter.

JHEP02(2011)105

(where the factor of -2 difference from eq. (1.1) is because J^μ_A is the right-handed minus the left-handed currents). In real-world QCD the up and down quark masses are very small, $m_{u,d} \simeq 2.0, 4.5$ MeV [39] and so in many situations one may neglect the explicit current nonconservation.

Neglecting the quark masses, the amplitude to evolve from state $|\psi_1(t_1)\rangle$ to state $|\psi_2(t_2)\rangle$ *times* the change in axial number is (in the Heisenberg picture)

$$A\Delta Q_{A,q} = 2\int_{t_1}^{t_2} dt \int d^3\boldsymbol{x} \langle\psi_2| \frac{g^2}{32\pi^2} F^a_{\mu\nu}\tilde{F}^{\mu\nu}_a(\boldsymbol{x},t)|\psi_1\rangle\,. \tag{2.3}$$

The probability of the process times the square of the change is

$$P(\Delta Q_{A,q})^2 = 4\int d^4X d^4Y \langle\psi_1| \frac{g^2}{32\pi^2} F^a_{\mu\nu}\tilde{F}^{\mu\nu}_a(X)|\psi_2\rangle\langle\psi_2| \frac{g^2}{32\pi^2} F^a_{\alpha\beta}\tilde{F}^{\alpha\beta}_a(Y)|\psi_1\rangle\,. \tag{2.4}$$

Summing over final states, $\sum_{\psi_2} |\psi_2\rangle\langle\psi_2| = 1$, we find

$$\langle(\Delta Q_{A,q})^2\rangle = 4\int d^4X d^4Y \langle\psi_1| \frac{g^2}{32\pi^2} F^a_{\mu\nu}\tilde{F}^{\mu\nu}_a(X) \frac{g^2}{32\pi^2} F^a_{\alpha\beta}\tilde{F}^{\alpha\beta}_a(Y)|\psi_1\rangle\,. \tag{2.5}$$

The mean squared change for a general density matrix ρ is found by replacing $(\langle\psi_1|\ldots|\psi_1\rangle)$ with $(\mathrm{Tr}\,\rho\ldots)$. Note that the operators here are not time-ordered; it is the Wightman correlator

$$G^>_{F\tilde{F}}(X,Y) \equiv \left\langle \frac{g^2}{32\pi^2} F^a_{\mu\nu}\tilde{F}^{\mu\nu}_a(X)\ \frac{g^2}{32\pi^2} F^a_{\alpha\beta}\tilde{F}^{\alpha\beta}_a(Y) \right\rangle \tag{2.6}$$

which is relevant here.

Eq. (2.5) holds for arbitrary density matrices including nonequilibrium density matrices. Here we will more modestly try to evaluate it for the thermal ensemble. Since the thermal ensemble is 4-translation invariant, the mean-squared $Q_{A,q}$ change is extensive in 4-volume and it is more useful to define a rate of change per 4-volume:

$$\begin{aligned} \langle(\Delta Q_{A,q})^2\rangle_{\text{therm.}} &= 4Vt\,\Gamma_{\text{sphal}}\,, \\ \Gamma_{\text{sphal}} &\equiv \int d^4X G^>_{F\tilde{F}}(X,0)\,. \end{aligned} \tag{2.7}$$

This is the same as the zero frequency and momentum limit of the momentum-space Wightman function

$$G^>_{F\tilde{F}}(P) \equiv \int d^4X e^{-iP\cdot X} G^>_{F\tilde{F}}(X,0)\,. \tag{2.8}$$

In defining the sphaleron rate in this way we have tacitly assumed that the generated $(Q_{A,q})$ value can persist without influencing the subsequent evolution of the system. Of course this is not true; a net abundance of $Q_{A,q}$ leads to chemical potentials for left and right handed quark number which will then energetically bias future topology change to allow that quark number to relax. Defining $Q_5 = \sum_q Q_{Aq}$ the total axial light quark charge, standard fluctuation-dissipation arguments [10, 40] show that

$$\frac{dQ_5}{dt} = -Q_5 \frac{(2N_{\text{f}})^2}{\chi_Q} \frac{\Gamma_{\text{sphal}}}{2T} \simeq -Q_5 \frac{6N_{\text{f}}}{N_{\text{c}}} \frac{\Gamma_{\text{sphal}}}{T^3}\,, \tag{2.9}$$

JHEP02(2011)105

where χ_Q is the susceptibility for Q_5 and in the last line we used the leading-order perturbative estimate $\chi_Q = N_{\rm f}\, N_{\rm c} T^2/3$. What this expression means is that any fluctuation-induced nonvanishing value for Q_5 will bias all subsequent topology changing processes, causing Q_5 to relax back to zero with fluctuations set by the susceptibility. This means that a fluctuation in topology of one sign will eventually be balanced by a fluctuation of the other sign with a time constant $\tau \sim 2T\chi_Q/(4N_{\rm f}{}^2\Gamma_{\rm sphal})$. To define the sphaleron rate we implicitly assume that this time scale is long compared to any microscopic time scales, and we implicitly cut off the time integration in eq. (2.7) on a timescale shorter than τ but longer than microscopic time scales. At weak coupling the longest microscopic time scale is $\sim 1/\alpha_{\rm s}^2 T$ while the relaxation time scale defined above is $\sim 1/\alpha_{\rm s}^5 T$ (as we shall see), so the separation of scales exists. The separation also exists at strong coupling in large $N_{\rm c}$ $\mathcal{N}$=4 SYM theory, where the sphaleron rate is $\Gamma_{\rm sphal} = (g^2 N_{\rm c})^2 T^4/256\pi^3 \sim N_{\rm c}^0$ [41], while $\chi_Q \sim N_{\rm c}^2 T^2$. Therefore $\tau \sim N_{\rm c}^2/T$ is large in the large number of colors limit.[4] However for $N_{\rm c} = 3$ ordinary QCD at $T \sim 200$MeV it is by no means clear that such a separation of scales exists, and it is possible that one cannot really define a sphaleron rate *per se*.

2.2 Relation to Euclidean correlation functions

We saw above that the sphaleron rate is set by the zero frequency and momentum limit of the $F\tilde{F}$ Wightman function. Naively one might think it is easy to determine the sphaleron rate from Euclidean correlation functions, which can be measured on the lattice. Indeed, in the late 1980's there were some misconceptions that such things should be possible, which were quashed by a paper by Arnold and McLerran [22]. Here we remind the reader how the sphaleron rate is related to Euclidean correlation functions, and why it would *not* be easy to determine it from Euclidean lattice data. Though the remarks here are rather generic to two-point functions and are well known, we review them in a little detail because we are not aware that they have been clearly discussed in this particular context.

The Wightman correlation function defined above is

$$G^{>}_{F\tilde{F}}(X) \equiv \mathrm{Tr}\, e^{-\beta H} e^{iHt} \frac{g^2}{32\pi^2} F^a_{\mu\nu} \tilde{F}^{\mu\nu}_a(\boldsymbol{x}) e^{-iHt} \frac{g^2}{32\pi^2} F^a_{\alpha\beta} \tilde{F}^{\alpha\beta}_a(0) \tag{2.10}$$

while the Euclidean correlation function is

$$G^{\rm E}_{F\tilde{F}}(\tau, \boldsymbol{x}) \equiv \mathrm{Tr}\, e^{-\beta H} e^{\tau H} \frac{g^2}{32\pi^2} F^a_{\mu\nu} \tilde{F}^{\mu\nu}_a(\boldsymbol{x}) e^{-\tau H} \frac{g^2}{32\pi^2} F^a_{\alpha\beta} \tilde{F}^{\alpha\beta}_a(0)\,, \tag{2.11}$$

defined on the range $0 < \tau < \beta$ and satisfying periodic boundary conditions, $G^{\rm E}(\beta, \boldsymbol{x}) = G^{\rm E}(0, -\boldsymbol{x}) = G^{\rm E}(0, \boldsymbol{x})$.[5] It is clear from the definitions that $G^{>}(t, \boldsymbol{x})$ is the analytic continuation $\tau \to it$ of $G^{\rm E}(\tau, \boldsymbol{x})$. In particular the equal-time value of $G^{>}$ equals the equal τ value of $G^{\rm E}$.

But what we want is the zero *Minkowski frequency* limit of $G^{>}$, and the frequency transforms of the two functions are *not* the same. Instead, the frequency-space transform

[4] The calculation is only valid in the limit $N_{\rm c} \gg (g^2 N_{\rm c}) \gg 1$. In this limit the relaxation time is parametrically large, while all microscopic timescales are $\sim T$.

[5] Note that $F\tilde{F}$ is a pseudoscalar. $G(-\boldsymbol{x})$ can be related to $G(\boldsymbol{x})$ by a rotation; parity is not involved.

JHEP02(2011)105

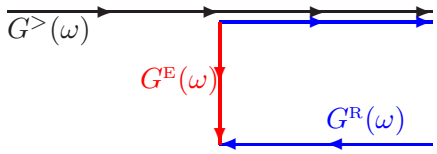

Figure 1. Integration contours in complex t plane for $G^{>}(\omega)$, $G^{\rm E}(\omega)$, and $G^{\rm R}(\omega)$ (the latter for $\mathrm{Im}(\omega) = 2\pi n$ only). Contour deformation turns $G^{\rm R}$, but not $G^{>}$, into $G^{\rm E}$.

of the Euclidean function continues to the retarded correlation function

$$\begin{aligned} G^{\rm R}_{F\tilde{F}}(t,\boldsymbol{x}) &\equiv \left\langle \left[\frac{g^2}{32\pi^2} F^a_{\mu\nu}\tilde{F}^{\mu\nu}_a(t,\boldsymbol{x})\,,\, \frac{g^2}{32\pi^2} F^a_{\alpha\beta}\tilde{F}^{\alpha\beta}_a(0,0) \right] \right\rangle \Theta(t) \\ &= \Theta(t)\left(G^{>}_{F\tilde{F}}(t,\boldsymbol{x}) - G^{<}_{F\tilde{F}}(t,\boldsymbol{x}) \right) . \end{aligned} \tag{2.12}$$

The reason why is illustrated in figure 1: first note that the frequency domain form of $G^{\rm R}$,

$$G^{\rm R}(\omega) = \int_0^\infty dt e^{i\omega t}\Big(G^{>}(t) - G^{<}(t) \Big) \tag{2.13}$$

is trivial to continue to complex ω with $\mathrm{Im}\,\omega > 0$. For purely imaginary $\omega = i\omega_{\rm E}$ with $\beta\omega_{\rm E} = 2\pi n$ it is

$$G^{\rm R}(i\omega_{\rm E}) = \int_0^\infty dt e^{i\omega_{\rm E} it} G^{>}(t) - \int_0^\infty dt e^{i\omega_{\rm E} it} G^{<}(t)\,. \tag{2.14}$$

But the KMS condition is that

$$\begin{aligned} G^{<}_{F\tilde{F}}(t) &\equiv \mathrm{Tr}\, e^{-\beta H} F\tilde{F} e^{iHt} F\tilde{F} e^{-iHt} \\ &= \mathrm{Tr}\, e^{-\beta H}\tilde{F} e^{-\beta H} e^{\beta H} e^{iHt} F\tilde{F} e^{-iHt} \qquad \text{(inserting } e^{\pm\beta H}\text{)} \\ &= \mathrm{Tr}\, e^{-\beta H}\, e^{\beta H} e^{iHt} F\tilde{F} e^{-iHt} e^{-\beta H} F\tilde{F} \qquad \text{(cyclicity of the trace)} \\ &= \mathrm{Tr}\, e^{-\beta H}\, e^{i(-i\beta+t)H} F\tilde{F} e^{-i(-i\beta+t)H} F\tilde{F} \\ &= G^{>}_{F\tilde{F}}(t - i\beta)\,. \end{aligned} \tag{2.15}$$

Substituting into eq. (2.14) and noting that $e^{i\omega_{\rm E}\beta} = 1$, we find

$$\begin{aligned} G^{\rm R}(i\omega_{\rm E}) &= \int_0^\infty dt e^{i\omega_{\rm E} it} G^{>}(t) - \int_{-i\beta}^{\infty - i\beta} dt e^{i\omega_{\rm E} it} G^{>}(t) \\ &= \int_0^{-i\beta} dt e^{i\omega_{\rm E} it} G^{>}(t) = -i\int_0^\beta d\tau e^{i\omega_{\rm E}\tau} G^{\rm E}(\tau) \equiv -iG^{\rm E}(\omega_{\rm E}) \end{aligned} \tag{2.16}$$

the Fourier (series) transform of the Euclidean function.

The conclusion is that, while Euclidean techniques determine $G^{>}(t = 0, \boldsymbol{x})$ in a straightforward way, the zero Euclidean frequency correlation function [the Euclidean topological susceptibility] corresponds to the zero Minkowski frequency, *retarded* function, not the zero frequency Wightman function. That is, the Euclidean, frequency-domain correlation function continues to a Minkowski, frequency domain function with the wrong operator ordering.

JHEP02(2011)105

The Euclidean function does have *some* relation to the Wightman function, through the Kramers-Kronig relations. Namely, defining

$$\sigma_{F\tilde{F}}(t) \equiv G^{>}(t) - G^{<}(t) \quad \Rightarrow \quad \sigma_{F\tilde{F}}(\omega) = (1 - e^{-\beta\omega})G^{>}(\omega) \simeq \beta\omega G^{>}(\omega)\,, \tag{2.17}$$

the retarded function at arbitrary complex frequency ω is determined by $\sigma(\omega')$ at real frequency by

$$G^{\rm R}_{F\tilde{F}}(\omega) = \int_{-\infty}^{\infty} \frac{d\omega'}{2\pi i} \frac{\sigma_{F\tilde{F}}(\omega')}{\omega' - \omega - i\epsilon}\,. \tag{2.18}$$

Evaluating for imaginary (Euclidean) ω and inverse transforming to τ,

$$G^{\rm E}_{F\tilde{F}}(\tau) = \int_{0}^{\infty} \frac{d\omega'}{\pi} \frac{\sigma_{F\tilde{F}} \cosh\Big(\omega'(\tau - \beta/2)\Big)}{\sinh \omega'\beta/2}\,. \tag{2.19}$$

Unfortunately, what we can measure on the lattice, $G^{\rm E}_{F\tilde{F}}(\tau)$, determines an integral over what we want, $\sigma_{F\tilde{F}}(\omega')$. To proceed further we would need some method to invert this integral relation. This problem has frustrated the evaluation of similar equilibration rates such as the electrical conductivity and the shear viscosity [42].

We now argue that the problems encountered in continuing $F\tilde{F}$ from lattice data are more severe than for continuing the correlation functions needed for conductivity or viscosity. The problem is that there is no local[6] lattice definition of the topological charge density operator $\frac{g^2}{32\pi^2}F^a_{\mu\nu}\tilde{F}^{\mu\nu}_a$ which satisfies the property that $\int d^4X \frac{g^2}{32\pi^2}F^a_{\mu\nu}\tilde{F}^{\mu\nu}_a$ over a compact 4-volume is topological (for a discussion see [43]). There *are* definitions of $\int d^4X \frac{g^2}{32\pi^2}F^a_{\mu\nu}\tilde{F}^{\mu\nu}_a$ which are topological (given some mild constraints on the smoothness of lattice fields) [44–47]. That means that there is no problem in principle with evaluating $G^{\rm E}_{F\tilde{F}}(\omega_{\rm E} = 0, \boldsymbol{p} = 0)$ or [given real-time lattice configurations] $G^{>}_{F\tilde{F}}(\omega = 0, \boldsymbol{p} = 0)$. But any attempt to compute $\int d^3\boldsymbol{x}\, G^{\rm E}_{F\tilde{F}}(\tau, \boldsymbol{x})$ relies on measuring $F\tilde{F}$ on a 3-D rather than 4-D surface, and so will necessarily be contaminated by either the non-topological or the non-local nature of the operators used in the evaluation. We believe that this additional complication will make $\Gamma_{\rm sphal}$ even harder than other transport coefficients to extract from Euclidean lattice calculations.

3 Effective theories and computation

As reviewed in the last section, the sphaleron rate is an intrinsically Minkowski quantity which cannot be evaluated with Euclidean methods. Because $\frac{g^2}{32\pi^2}F^a_{\mu\nu}\tilde{F}^{\mu\nu}_a$ is a total derivative, the sphaleron rate is a strictly nonperturbative quantity which vanishes to all orders of perturbation theory. Therefore its evaluation requires nonperturbative, Minkowski tools. These are in very short supply. To our knowledge, we have only two approaches to measuring the sphaleron rate:

[6] By local here we mean that the operator has compact support which is independent of the lattice configuration, i.e. it stretches for a fixed finite number of lattice spacings. It may be possible to meet our requirements with an operator which falls off exponentially with lattice distance, but only if the exponential falloff rate is conditional on the smoothness of the lattice configuration.

JHEP02(2011)105

- In certain gauge theories which possess gravity duals (generally highly supersymmetric theories) there are holographic methods which allow the sphaleron rate to be related to string theory correlators. These can be evaluated on the string theory side in the strong-coupling, large N_c limit of the gauge theory, see [41]. The results are suggestive but do not apply to ordinary QCD.

- In the weak coupling (high temperature) domain, the only nonperturbative physics which is not exponentially suppressed is essentially *classical field* physics. Therefore it should be possible to evaluate the sphaleron rate by studying classical field dynamics as an effective IR description [23, 48].

In this work we will follow this second approach. This method has already been pushed to its logical conclusions for the electroweak $\mathrm{SU_L}(2)$ sector [25–32]. Here we briefly review what that literature has found.

3.1 Bödeker's effective theory

Naively, the infrared fields in a weakly coupled quantum field theory of massless degrees of freedom should obey the classical equations of motion, in our case

$$D_\nu F^{\nu\mu} = -J^\mu \tag{3.1}$$

with the initial field values drawn from a statistical distribution of classical fields weighted by the Boltzmann factor $\exp(-E/T)$. Bödeker has shown [49] that the first corrections to this picture enter at order $\hbar^2$ *except* for the possibility of large (loop) corrections in the ultraviolet. That is, J^μ is a composite operator so an infrared field component could arise from the overlap of UV fluctuations with almost the same wave number, e.g. $J^\mu(k) = \int_p \bar\psi(-p)\gamma^\mu\psi(p+k)$. These fields can in turn be correlated with past and present IR gauge fields, leading to effective modifications of the infrared gauge dynamics. Such large modifications of the IR dynamics do indeed occur; they are just the Hard Thermal Loops of Braaten and Pisarski [50, 51].

The sphaleron rate depends in particular on the behavior of transverse (magnetic) fields in the deep infrared. In this case the Hard Thermal Loops have a particularly simple interpretation; the spatial current in eq. (3.1) is determined by Ohm's law and the color conductivity; writing noncovariantly, the spatial components read [31]

$$D_j F_{ji} + D_t E_i = -J_i \quad = -\sigma E_i + \zeta_i \tag{3.2}$$

with σ the color conductivity and ζ_i a Langevin noise source which maintains thermal equilibrium. In general the color conductivity is frequency and momentum dependent, but for the most infrared fields of relevance to the sphaleron rate, "color randomization" means that σ should be essentially a constant of value [30, 31, 34, 35]

$$\sigma^{-1} = \frac{3N_c g^2 T}{4\pi m_D^2}\left[\ln\frac{m_D}{\gamma} + 3.0410\right] ,$$
$$\gamma = \frac{N_c g^2 T}{4\pi}\left(\ln\frac{m_D}{\gamma} + \mathcal{O}(1)\right) , \tag{3.3}$$
$$m_D^2 = \frac{2N_c + N_f}{6} g^2 T^2 . \tag{3.4}$$

JHEP02(2011)105

(Physically, the conductivity $\sigma = m_{\rm D}^2/3\gamma$ is a polarizability times a mean free path. The factor of $m_{\rm D}^2/3$ is the polarizability and $1/\gamma$ is the mean free path for color randomization.) This conductivity is parametrically large and allows one to neglect the $D_t E_i$ term in eq. (3.2) relative to the σE_i term, yielding the effective description

$$D_j F_{ji} = -\sigma E_i + \zeta_i \,, \qquad \int dt \zeta_i(\boldsymbol{x},t)\zeta_j(y,0) = 2\sigma T \delta_{ij}\delta^3(\boldsymbol{x}-\boldsymbol{y}) \,. \tag{3.5}$$

The normalization of ζ_i ensures that the fields are distributed according to the classical thermal ensemble, as required by the fluctuation dissipation theorem [31].

Note that in finding this effective description and in particular that σ is a constant, we have made an expansion (to second order [34, 35]) in $\ln(1/g)$ the logarithm of the inverse coupling. While the numerical coefficient 3.0410 stabilizes this expansion somewhat, it is a rather marginal expansion and one should expect rather large corrections at physically interesting couplings. Nevertheless we first pursue this approach because the effective theory involved, eq. (3.5), is a Langevin equation with very good mathematical properties. In particular, unlike eq. (3.1), eq. (3.5) possesses *dynamics* which have a well defined limit as the UV regulator is taken to infinity [31, 33]. Therefore it can be implemented on a lattice, and the lattice spacing $a \to 0$ limit may be taken to obtain a well defined limit for $\Gamma_{\rm sphal}$ in this effective theory.

3.2 Numerical implementation

Our implementation of SU(3) gauge theory on a lattice is standard, and we measure Chern-Simons number using the algorithm of [52], which extends easily to general SU($N_{\rm c}$). We do *not* follow the implementation of Langevin dynamics from [33], however, so we will make some remarks about how we do implement Langevin dynamics. First, it is convenient to rescale the time variable in eq. (3.5) to conventional Langevin time

$$\tau_{\rm L} = t/\sigma \tag{3.6}$$

which, note, has units of time squared. In terms of this Langevin time the fields evolve according to conventional Langevin equations; in $A_0 = 0$ gauge,

$$\partial_{\tau_{\rm L}} A_i = -D_j F_{ji} + \zeta_i' = -\frac{\partial H}{\partial A_i} + \zeta_i' \,, \qquad \int d\tau_{\rm L} \zeta_i'(\tau_{\rm L},y)\zeta_j'(x,0) = 2T\delta_{ij}\delta^3(\boldsymbol{x}-\boldsymbol{y}) \,. \tag{3.7}$$

The sphaleron rate $\Gamma_{\rm L} = \int d\tau_{\rm L} \int d^3\boldsymbol{x} F\tilde{F}(\tau_{\rm L},\boldsymbol{x}) F\tilde{F}(0,0)$ obtained in this theory is related to that obtained using eq. (3.5) by a factor of σ.

Any numerical implementation of eq. (3.7) requires discretization of $\tau_{\rm L}$ into finite steps. The challenge is that larger steps result in a faster algorithm but may have larger numerical errors; in particular the sphaleron rate scales as T^4 and so is sensitive to any correction which shifts the thermodynamics. Therefore we particularly want an algorithm which respects the correct thermodynamics to good, controllable accuracy. Our choice is to implement eq. (3.7) as a series of short Hamiltonian trajectories of length $t_{\rm H}$, with the electrical field drawn randomly from a Gaussian ensemble at the beginning of each trajectory. To

JHEP02(2011)105

see how this reproduces eq. (3.7), consider the following Hamilton's equations (in $A_0 = 0$ gauge, which we choose for explanatory convenience):

$$\begin{aligned} \partial_t E_i &= -\frac{\partial H}{\partial A_i}\,, \\ \partial_t A_i &= E_i\,, \\ \langle E_i(\boldsymbol{x}, t=0) E_j(\boldsymbol{y}, t=0)\rangle &= T\delta_{ij}\delta^3(\boldsymbol{x}-\boldsymbol{y})\,. \end{aligned} \tag{3.8}$$

(The lattice implementation of these equations is known, see for instance [23] but note that in the above we do *not* enforce Gauss' Law.) To second order in small $t_{\rm H}$, the change in A_i is found to be

$$A_i(\boldsymbol{x}, t_{\rm H}) - A_i(\boldsymbol{x}, 0) = E_i(\boldsymbol{x}) t_{\rm H} - \frac{\partial H}{\partial A_i}\frac{t_{\rm H}^2}{2} + \mathcal{O}({t_{\rm H}}^3)\,. \tag{3.9}$$

This is the same as eq. (3.7) if we interpret $\tau_{\rm L} = t_{\rm H}^2/2$. Hence, a randomization of the E fields followed by an evolution of time $t_{\rm H}$ corresponds to an evolution of $\tau_{\rm L} = t_{\rm H}^2/2$ units of Langevin dynamics up to higher order in $t_{\rm H}$ corrections. Higher order corrections are inevitable in a discretization of Langevin dynamics, and in this case we know that any corrections to the interpretation of the algorithm in terms of Langevin dynamics must enter at even powers in $t_{\rm H}$, since the algorithm described is actually t-even. In practice we measure $\Gamma_{\rm L}$ for two or more values of $t_{\rm H}$ and make an extrapolation to the small $t_{\rm H}$ limit, based on values no longer than one lattice unit. We also apply the known $\mathcal{O}(a)$ lattice-continuum corrections to the lattice spacing [53] and to the time scale t, which is known for Hamiltonian dynamics [33].

4 Weak-coupling results

We want the large volume, small lattice-spacing limit and our goal is a few percent precision. There are many systematic limits to consider; lattice spacing $a \to 0$, volume $V \to \infty$, refresh frequency $t_{\rm H} \to 0$, leapfrog timestep size, and parameters of our $N_{\rm CS}$ measuring method. Some of these are simple to control; we can check systematically that our $N_{\rm CS}$ measurement is topological because our method is "calibrated" with integrations to the vacuum [52]. Errors associated with the leapfrog step size are quadratic in the step; we compared step sizes of 0.2 and 0.1 and found a $4 \pm 2\%$ change in $\Gamma_{\rm L}$. Hence the difference between 0.1 and 0 is $1.3 \pm 0.7\%$ which is acceptably small. We typically extrapolate over two $t_{\rm H}$ values, $t_{\rm H} = a$ and $t_{\rm H} = a/2$. The resulting $\Gamma_{\rm L}$ generally differ by less than 10%, so higher orders in the extrapolation should be at the 1% level and therefore negligible.

Next we consider the extrapolation to infinite volume. The good news is that 3-D SU($N_{\rm c}$) gauge theory has a mass gap, so the approach to large volume behavior is expected to improve exponentially in box length for boxes much larger than the correlation length. In practice we measure the sphaleron rate at fixed lattice spacing a (technically, at a fixed value of the dimensionless ratio $g^2 aT$) for several volumes to see what volume is sufficient to achieve the large volume limit. This was first done by Ambjørn and Krasnitz [25, 26]. Our results, shown in figure 2, indicate that the volume dependence of the sphaleron rate

JHEP02(2011)105

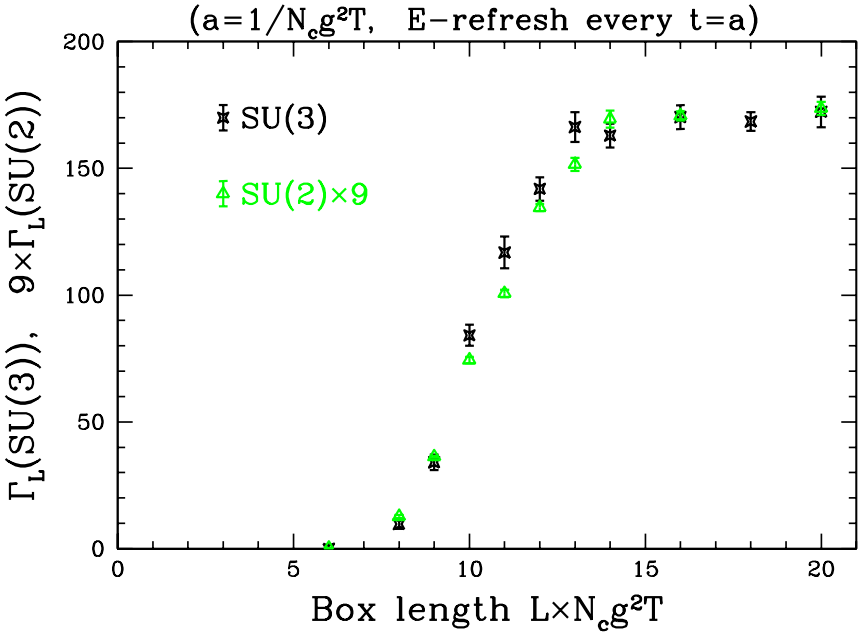

Figure 2. (Color online) Volume dependence of the sphaleron rate in Langevin dynamics, determined on lattices with spacing $a = 1/N_c g^2 T$, for SU(2) and SU(3). Errors are statistical only; data are not extrapolated to $t = 0$ or $a = 0$. Using the indicated scaling, the SU(2), SU(3) behaviors look very similar; the rate saturates around $L = 15/N_c g^2 T$.

in SU(2) and SU(3) gauge theory are almost identical *if* we scale the box length by $N_c g^2 T$, not $g^2 T$. We also see that the sphaleron rate increases with volume but saturates around $L = 15/N_c g^2 T$. Therefore we should make sure $L > 15/N_c g^2 T$ to be in the infinite volume limit. We therefore use $L \geq 18/N_c g^2 T$ in what follows.[7]

Finally, we consider the small lattice spacing a limit. Since the numerical effort required to get the same level of statistical significance increases as a^{-5}, we should try to understand this limit as well as possible. We know that, at the level of the thermodynamics of the system, there are corrections already at the $\mathcal{O}(a)$ level. These are well understood and amount to an effective rescaling of the lattice spacing [53]:

$$\frac{1}{a_{\rm corrected}} = \frac{1}{a_{\rm bare}} - N_c g^2 T \times \begin{cases} 0.07918 & \mathrm{SU}(2) \\ 0.10232 & \mathrm{SU}(3) \\ 0.12084 - 1/(6N_c^2) & \mathrm{SU}(N_c) \end{cases} \tag{4.1}$$

Choosing $a < 1/N_c g^2 T$ is then sufficient to push this correction under 10%. There are unknown $\mathcal{O}(a^2)$ corrections which are presumably of order the square of this size, so $a < 1/N_c g^2 T$ would leave of order 1% unknown corrections to the effective lattice spacing. But the scaling between lattice and continuum Langevin diffusion rates involves a^5, so even a 1% error in a leads to a 5% error in the diffusion rate, which is not acceptable. There are also

[7] Note that using very large volumes is not helpful; since the measurement of $N_{\rm CS}$ is global over the lattice, there is no gain in statistics as the lattice volume increases, while the numerical effort increases with volume.

JHEP02(2011)105

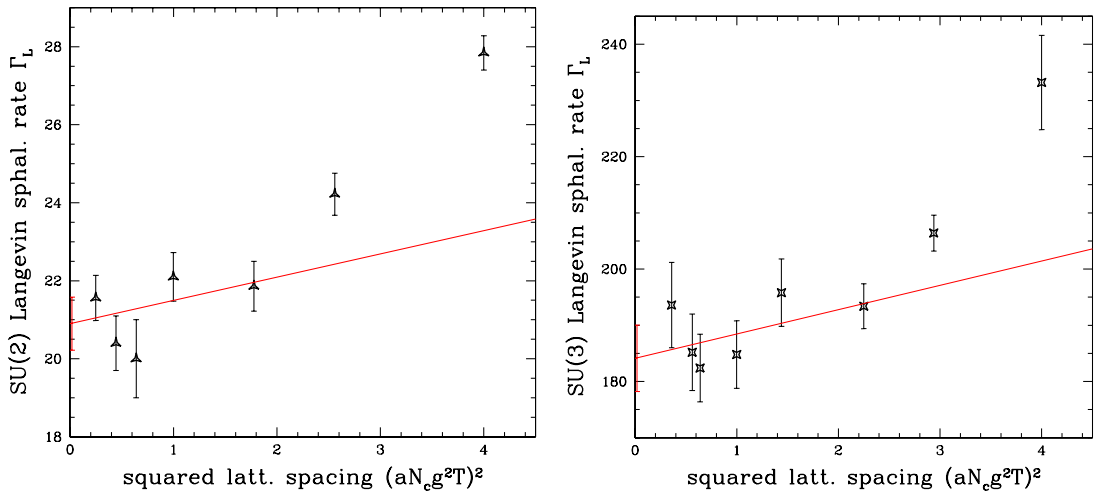

Figure 3. (color online) Finite lattice spacing extrapolation of SU(2) [left] and SU(3) [right] lattice Langevin sphaleron rate. The two largest lattice-spacing points were not used in the extrapolation.

Group	aN_cg^2T	Γ_L	Group	aN_cg^2T	Γ_L
SU(3)	2.00	233.2 ± 8.4	SU(2)	2.00	27.84 ± 0.44
SU(3)	1.72	206.4 ± 3.2	SU(2)	1.60	24.22 ± 0.54
SU(3)	1.50	193.4 ± 4.0	SU(2)	1.33	21.86 ± 0.64
SU(3)	1.20	195.8 ± 6.0	SU(2)	1.00	22.10 ± 0.62
SU(3)	1.00	184.8 ± 6.0	SU(2)	0.80	20.00 ± 1.00
SU(3)	0.80	182.4 ± 6.0	SU(2)	0.67	20.40 ± 0.70
SU(3)	0.75	185.2 ± 6.8	SU(2)	0.50	21.56 ± 0.58
SU(3)	0.60	193.6 ± 7.6			

Table 1. Numerical results for the sphaleron rate under Langevin diffusion, for SU(2) and SU(3) gauge theory and several lattice spacings. Each result is taken at a volume with $L \geq 18/N_c g^2 T$ and is already extrapolated to zero t_H; systematic errors from these extrapolations are smaller than the indicated statistical errors.

other unknown $\mathcal{O}(a^2)$ corrections which cannot necessarily be represented as a rescaling of a or of τ_L. Hence we should try to get to lattices which are somewhat smaller than $a = 1/N_c g^2 T$, and to perform an $a \to 0$ extrapolation over the remaining a^2 corrections.

Our data for Γ_L as a function of a^2 is presented in figure 3 and table 1. The two largest-a lattices used are not included in the fit, because the corrections are too large (the fit becomes poor) and because the behavior of N_{CS} is not yet strictly topological (the N_{CS} measuring algorithm sometimes shows an inconsistency in which $\int F\tilde{F}$ from vacuum, along the Langevin history, and back to vacuum is far from an integer). To convert the extrapolated value into the result in eq. (1.3), we multiply by $(3N_c/4\pi)$ as indicated in eq. (3.3), eq. (3.6). As a check on our Langevin dynamics method, we have also repeated the calculation of the SU(2) sphaleron rate originally performed in [33]; we find that the coefficient in eq. (1.3) for SU(2) is 10.0 ± 0.3, in agreement with 10.8 ± 0.7 found there.

JHEP02(2011)105

Colors N_c	Coeff. in eq. (1.3)	Coeff. in eq. (4.2)
2	9.53 ± 0.14	$0.198 \pm .003$
3	127.8 ± 4.0	$0.197 \pm .006$
5	2790 ± 70	$0.186 \pm .005$
8	51300 ± 3100	$0.199 \pm .012$

Table 2. The Langevin equation $N_{\rm CS}$ diffusion rate as a function of the number of colors N_c, for a fixed lattice spacing $a = 0.8/N_c g^2 T$ and E-field refresh rate $t_H = a$.

In [36] one of us speculated that Γ_L should scale with N_c as $\frac{N_c^2-1}{N_c^2}(N_c\alpha)^5 T^4$, and in particular

$$\Gamma_{\rm sphal} = \kappa' \left(\frac{N_c g^2 T^2}{m_D^2}\right) \left(\ln \frac{m_D}{\gamma} + 3.0410\right) (N_c^2-1) N_c^3 \alpha_s^5 T^4 \,, \tag{4.2}$$

with $\kappa' \sim 0.24$. We have investigated this speculation by computing the sphaleron rate at a single value of $a = 0.8/N_c g^2 T$ for several values of N_c, shown in table 2. The data in the table are also not extrapolated to $t_H = 0$ but are computed at $t_H = a$. Extrapolating by assuming that the a and t_H scaling are the same as for $N_c = 2, 3$, the a^2 correction lowers the rate by 1.8% and the $t_H \to 0$ correction raises the rate 9% so we find $\kappa' = 0.21 \pm .01$, as quoted in eq. (1.6).

5 Finite-coupling desperation

Our calculation has made a strict weak-coupling expansion, which is really two approximations. First, in writing the theory in terms of classical fields on the lattice, we assume the nonperturbative IR dynamics is essentially classical. Second, by implementing Langevin dynamics, we assume that color conductivity is large and wavelength independent. We cannot relax the first approximation without losing our computational method altogether. But we can relax the second approximation and allow the conductivity to be finite, by studying the theory with Hamiltonian dynamics [23, 25, 26]. This allows us access to "intermediate" couplings, though with larger theoretical errors.

At weak coupling, the continuum theory has three parametric length scales:

- The length scale $1/T$, where most thermal degrees of freedom reside,
- The length scale $1/\sqrt{N_c}\, gT$ associated with screening phenomena,
- The length scale $1/N_c g^2 T$, where physics is nonperturbative.

The corresponding scales for the Hamiltonian lattice theory are a, $\sqrt{a/N_c g^2 T}$, and $1/N_c g^2 T$. Only two of these scales are relevant for the dynamics of topology change; the $1/N_c g^2 T$ scale where the nonperturbative physics occurs, and the $1/\sqrt{N_c}\, gT$ "screening" scale which influences the dynamics of the IR scale. On the lattice one does not choose a, g^2, and T separately; one controls the dimensionless ratio $aN_c g^2 T$ (often written $2N_c^2/\beta_L$). But this choice can be paraphrased as a choice for a finite value of $g^2 N_c$, as we now show.

JHEP02(2011)105

Since the sphaleron rate involves the evolution of infrared magnetic fields, the relevant feature of $1/gT$ physics is the "damping rate" for the evolution of magnetic fields [38]. In the continuum this is proportional to $m_{\rm D}^2$. On the lattice it is proportional to an integral which diverges as $1/a$.[8] Equating them, we find [38]

$$k\gamma_{\rm contin} = \frac{(2N_{\rm c}+N_{\rm f})\pi g^2 T^2}{24} = k\gamma_{\rm latt} = \frac{2.14988\pi N_{\rm c} g^2 T}{8\pi a}\,, \tag{5.1}$$

which relates the screening scales of the lattice and continuum theories. Re-organizing, we can determine g^2 in terms of $(aN_{\rm c}g^2T)$:

$$\frac{2.14988\times 3}{\pi\frac{2N_{\rm c}+N_{\rm f}}{N_{\rm c}}} N_{\rm c} g^2 = aN_{\rm c}g^2T \quad\Rightarrow\quad \frac{g^2}{4\pi} = \frac{2N_{\rm c}+N_{\rm f}}{12N_{\rm c}^2(2.14988)}(aN_{\rm c}g^2T)\,. \tag{5.2}$$

We use this relation to convert a value of the lattice spacing — really, of $aN_{\rm c}g^2T$ — into an equivalent value of $\alpha_{\rm s} = g^2/4\pi$.

In Hamiltonian simulations of this sort, we measure the number of topology changes per unit of lattice spacetime volume. That is, $\Gamma = \langle(\Delta N_{\rm CS})^2\rangle/Vt$ and V, t are measured in terms of a^3 and a respectively. Using the known value of $aN_{\rm c}g^2T$, we can convert this into units of $\alpha_{\rm s}^4T^4$, so we determine $\Gamma = (\text{pure number})(\alpha_{\rm s}T)^4$. For direct comparison with our results using Langevin dynamics, it would be convenient to multiply and divide by an extra power of $\alpha_{\rm s}$, writing one explicitly and incorporating the other into the pure number. However, as eq. (5.2) shows, the value of $\alpha_{\rm s}$ depends not only on the lattice spacing (really $aN_{\rm c}g^2T$), but also on the number of fermionic species, that is, on the matter content. Therefore, we can express our answers in units of $\alpha_{\rm s}^4T^4$ in a way which is easy to apply to different matter contents, but to write our results in terms of $\alpha_{\rm s}^5T^4$ requires a seperate expression for each possible matter content. Therefore we will present our results for the sphaleron rate estimated using Hamiltonian lattice dynamics in terms of $\alpha_{\rm s}^4T^4$.

Table 3 presents our results for the sphaleron rate under Hamiltonian dynamics. The largest value of $aN_{\rm c}g^2T$ corresponds to the point where we can barely distinguish topological behavior on the lattice. For this value, the infinite volume limit was achieved with a lattice 8 on a side! For $\alpha_{\rm s}$ larger than this corresponding value, our ability to guess the strong sphaleron rate gets even weaker; we must extrapolate based on the behavior shown in the table. This corresponds to the case relevant for heavy ion collisions. The figure also shows the performance of the leading-log expansion, that is, the guess for the sphaleron rate using eq. (1.3) together with the matching for the Debye screening scale from eq. (5.2). The leading-log (Bödeker effective theory) approach reproduces the lattice Hamiltonian result for the finest lattices but is rather far off for the coarsest lattices, showing that the evolution is not overdamped for such coarse lattice spacing (large $\alpha_{\rm s}$).

[8] In studying the SU(2) sphaleron rate, where the gauge coupling is small, it is convenient to add "extra" degrees of freedom to the lattice, as done in [28, 32]. This effectively shortens the screening length scale on the lattice, which is the same as effectively making the coupling smaller. Since we want to explore the largest possible couplings, this is the opposite of what we want, which is why we consider the pure classical lattice theory without additional degrees of freedom.

JHEP02(2011)105

$aN_c g^2 T$	α_s(0 flavor)	α_s(3 flavor)	$\Gamma_{\rm sphal}/\alpha_s^4 T^4$	$\Gamma_{\rm sphal}/\alpha_s^4 T^4$ from eq. (1.3)
2.40	0.062	0.093	17.28 ± 0.30	27.7
2.00	0.052	0.078	14.06 ± 0.20	23.5
1.72	0.044	0.066	12.60 ± 0.27	20.5
1.50	0.039	0.058	11.45 ± 0.26	18.2
1.20	0.031	0.047	10.41 ± 0.22	14.9
1.00	0.026	0.039	9.18 ± 0.23	12.7
0.75	0.019	0.029	8.51 ± 0.16	9.8
0.60	0.016	0.023	7.81 ± 0.20	8.0

Table 3. SU(3) sphaleron rate under Hamiltonian dynamics, and its interpretation in terms of α_s for the 0-flavor and 3-flavor theories. Errors shown are statistical, and are dwarfed by much larger theoretical errors in equating lattice and continuum theories, which we have not estimated. We also show the result implied by eq. (1.3), which works well at the smallest lattice spacings but is a poor description for the coarsest lattices.

6 Discussion

We have computed the sphaleron rate in SU(3) gauge theory at weak coupling. In the weak coupling limit, there is a rigorous relation between the sphaleron rate and the topological diffusion rate for classical lattice gauge theory under Langevin dynamics, which we have computed with few-% error bars. We have also shown that the N_c-dependence for the sphaleron rate has a surprisingly simple and intuitive behavior. Our analysis of Hamiltonian dynamics on coarser lattices suggests that this Bödeker effective description only works at very small values of α_s. While it should apply for the SU(2) electroweak sector at all physically interesting temperatures, and for QCD at GUT scale temperatures, it is not a successful description of QCD at electroweak temperatures.

For applications to electroweak baryogenesis, we need the strong sphaleron rate in an $N_f = 6$ theory with $\alpha_s \sim 0.1$. The value of α_s for $N_f = 6$ is twice the value for $N_f = 0$, so this corresponds roughly to our $(aN_c g^2 T) = 2$ data point in table 3; the strong sphaleron rate relevant at the electroweak scale is approximately (note, written in terms of α_s^4 not α_s^5)

$$\Gamma_{\rm strong\,sphal}(N_f = 6, \alpha_s \sim 0.1) \simeq 14 \alpha_s^4 T^4 \,. \tag{6.1}$$

It is difficult to assign theoretical error bars to this estimate but they should be rather large; the relevant lattice spacing is so large that the topological nature of the $F\tilde{F}$ measurement is barely under control, and the lattice spacing corrections discussed earlier are not small. It is also not clear that the lattice field dynamics are a good description of the continuum, not-so-small coupling dynamics. We only have rigorous arguments that they agree for small coupling.[9] The continuum dynamics have $\mathcal{O}(g)$ (technically $\mathcal{O}(N_c g^2 T/m_D)$) corrections, the lattice dynamics have $\mathcal{O}(\sqrt{N_c g^2 a T})$ corrections, and there is no guarantee that they are the same (see for instance [54]). Therefore we expect at least $\mathcal{O}(50\%)$ systematic corrections to this result.

[9] Actually even the subleading in log correction 3.041 of eq. (1.3) will be different on the lattice. The lattice value for this constant has not been computed.

JHEP02(2011)105

Unfortunately, the coupling values $\alpha_s \sim 1/3$ relevant for heavy ion physics correspond to lattices too coarse for any study of topology to be successful. Therefore the best we can do is to extrapolate our existing results towards this regime. Plotting the points appearing in table 3, and putting a ruler through all but the last point, one extrapolates that, at $\alpha_s = 0.3$, $\Gamma_{\rm sphal} \sim 40\alpha_s^4 T^4$. But this extrapolation extends far beyond the range where we have "data" and cannot be taken seriously. It is not clear to us how to proceed at such large couplings; as we have argued, analytic continuation from Euclidean lattice calculations seems to be even more difficult than for other transport coefficients. But at least the behavior at the electroweak temperature scale, and at higher temperatures, is under some control.

Acknowledgments

We would like to thank Dima Kharzeev, for stimulating us to revisit this issue after so many years. This work was supported in part by the Natural Sciences and Engineering Research Council of Canada.

References

[1] A.A. Belavin, A.M. Polyakov, A.S. Schwartz and Y.S. Tyupkin, *Pseudoparticle solutions of the Yang-Mills equations*, *Phys. Lett.* **B 59** (1975) 85 [SPIRES].

[2] S.L. Adler, *Axial vector vertex in spinor electrodynamics*, *Phys. Rev.* **177** (1969) 2426 [SPIRES].

[3] J.S. Bell and R. Jackiw, *A PCAC puzzle: $\pi 0 \to \gamma\gamma$ in the σ-model*, *Nuovo Cim.* **A 60** (1969) 47 [SPIRES].

[4] G. 't Hooft, *Computation of the quantum effects due to a four-dimensional pseudoparticle*, *Phys. Rev.* **D 14** (1976) 3432 [*Erratum ibid.* **D 18** (1978) 2199] [SPIRES].

[5] F.R. Klinkhamer and N.S. Manton, *A Saddle Point Solution in the Weinberg-Salam Theory*, *Phys. Rev.* **D 30** (1984) 2212 [SPIRES].

[6] V.A. Kuzmin, V.A. Rubakov and M.E. Shaposhnikov, *On the Anomalous Electroweak Baryon Number Nonconservation in the Early Universe*, *Phys. Lett.* **B 155** (1985) 36 [SPIRES].

[7] P.B. Arnold and L.D. McLerran, *Sphalerons, Small Fluctuations And Baryon Number Violation In Electroweak Theory*, *Phys. Rev.* **D 36** (1987) 581 [SPIRES].

[8] V.A. Rubakov and M.E. Shaposhnikov, *Electroweak baryon number non-conservation in the early universe and in high-energy collisions*, *Usp. Fiz. Nauk* **166** (1996) 493 [*Phys. Usp.* **39** (1996) 461] [hep-ph/9603208] [SPIRES].

[9] J.M. Cline, *Baryogenesis*, hep-ph/0609145 [SPIRES].

[10] G.F. Giudice and M.E. Shaposhnikov, *Strong sphalerons and electroweak baryogenesis*, *Phys. Lett.* **B 326** (1994) 118 [hep-ph/9311367] [SPIRES].

[11] P. Huet and A. E. Nelson, *Electroweak baryogenesis in supersymmetric models*, *Phys. Rev.* **D 53** (1996) 4578 [hep-ph/9506477] [SPIRES].

JHEP02(2011)105

[12] J.M. Cline, M. Joyce and K. Kainulainen, *Supersymmetric electroweak baryogenesis in the WKB approximation*, *Phys. Lett.* **B 417** (1998) 79 [*Erratum ibid.* **B 448** (1999) 321] [hep-ph/9708393] [SPIRES].

[13] D.J.H. Chung, B. Garbrecht, M.J. Ramsey-Musolf and S. Tulin, *Supergauge interactions and electroweak baryogenesis*, *JHEP* **12** (2009) 067 [arXiv:0908.2187] [SPIRES].

[14] PHENIX collaboration, K. Adcox et al., *Formation of dense partonic matter in relativistic nucleus nucleus collisions at RHIC: Experimental evaluation by the PHENIX collaboration*, *Nucl. Phys.* **A 757** (2005) 184 [nucl-ex/0410003] [SPIRES].

[15] B.B. Back et al., *The PHOBOS perspective on discoveries at RHIC*, *Nucl. Phys.* **A 757** (2005) 28 [nucl-ex/0410022] [SPIRES].

[16] BRAHMS collaboration, I. Arsene et al., *Quark Gluon Plasma an Color Glass Condensate at RHIC? The perspective from the BRAHMS experiment*, *Nucl. Phys.* **A 757** (2005) 1 [nucl-ex/0410020] [SPIRES].

[17] STAR collaboration, J. Adams et al., *Experimental and theoretical challenges in the search for the quark gluon plasma: The STAR collaboration's critical assessment of the evidence from RHIC collisions*, *Nucl. Phys.* **A 757** (2005) 102 [nucl-ex/0501009] [SPIRES].

[18] D.E. Kharzeev, L.D. McLerran and H.J. Warringa, *The effects of topological charge change in heavy ion collisions: 'Event by event P and CP-violation'*, *Nucl. Phys.* **A 803** (2008) 227 [arXiv:0711.0950] [SPIRES].

[19] K. Fukushima, D.E. Kharzeev and H.J. Warringa, *The Chiral Magnetic Effect*, *Phys. Rev.* **D 78** (2008) 074033 [arXiv:0808.3382] [SPIRES].

[20] STAR collaboration, B.I. Abelev et al., *Observation of charge-dependent azimuthal correlations and possible local strong parity violation in heavy ion collisions*, *Phys. Rev.* **C 81** (2010) 054908 [arXiv:0909.1717] [SPIRES].

[21] S.A. Voloshin, *Testing the Chiral Magnetic Effect with Central $U+U$ collisions*, *Phys. Rev. Lett.* **105** (2010) 172301 [arXiv:1006.1020] [SPIRES].

[22] P.B. Arnold and L.D. McLerran, *The Sphaleron Strikes Back*, *Phys. Rev.* **D 37** (1988) 1020 [SPIRES].

[23] J. Ambjørn, T. Askgaard, H. Porter and M.E. Shaposhnikov, *Sphaleron transitions and baryon asymmetry: A Numerical real time analysis*, *Nucl. Phys.* **B 353** (1991) 346 [SPIRES].

[24] D. Bödeker, L.D. McLerran and A.V. Smilga, *Really computing nonperturbative real time correlation functions*, *Phys. Rev.* **D 52** (1995) 4675 [hep-th/9504123] [SPIRES].

[25] J. Ambjørn and A. Krasnitz, *The classical sphaleron transition rate exists and is equal to* $1.1(\alpha_w T)^4$, *Phys. Lett.* **B 362** (1995) 97 [hep-ph/9508202] [SPIRES].

[26] J. Ambjørn and A. Krasnitz, *Improved determination of the classical sphaleron transition rate*, *Nucl. Phys.* **B 506** (1997) 387 [hep-ph/9705380] [SPIRES].

[27] G.D. Moore and N. Turok, *Lattice Chern-Simons number without ultraviolet problems*, *Phys. Rev.* **D 56** (1997) 6533 [hep-ph/9703266] [SPIRES].

[28] G.D. Moore, C.-r. Hu and B. Müller, *Chern-Simons number diffusion with hard thermal loops*, *Phys. Rev.* **D 58** (1998) 045001 [hep-ph/9710436] [SPIRES].

[29] P.B. Arnold, D. Son and L.G. Yaffe, *The hot baryon violation rate is* $O(\alpha_w^5 T^4)$, *Phys. Rev.* **D 55** (1997) 6264 [hep-ph/9609481] [SPIRES].

JHEP02(2011)105

[30] D. Bödeker, *On the effective dynamics of soft non-abelian gauge fields at finite temperature*, *Phys. Lett.* **B 426** (1998) 351 [hep-ph/9801430] [SPIRES].

[31] P.B. Arnold, D.T. Son and L.G. Yaffe, *Hot B violation, color conductivity and* $\log(1/\alpha)$ *effects*, *Phys. Rev.* **D 59** (1999) 105020 [hep-ph/9810216] [SPIRES].

[32] D. Bödeker, G.D. Moore and K. Rummukainen, *Chern-Simons number diffusion and hard thermal loops on the lattice*, *Phys. Rev.* **D 61** (2000) 056003 [hep-ph/9907545] [SPIRES].

[33] G.D. Moore, *The sphaleron rate: Boedeker's leading log*, *Nucl. Phys.* **B 568** (2000) 367 [hep-ph/9810313] [SPIRES].

[34] P.B. Arnold and L.G. Yaffe, *Non-perturbative dynamics of hot non-Abelian gauge fields: Beyond leading log approximation*, *Phys. Rev.* **D 62** (2000) 125013 [hep-ph/9912305] [SPIRES].

[35] P.B. Arnold and L.G. Yaffe, *High temperature color conductivity at next-to-leading log order*, *Phys. Rev.* **D 62** (2000) 125014 [hep-ph/9912306] [SPIRES].

[36] G.D. Moore, *Do we understand the sphaleron rate?*, hep-ph/0009161 [SPIRES].

[37] G.D. Moore, *Computing the strong sphaleron rate*, *Phys. Lett.* **B 412** (1997) 359 [hep-ph/9705248] [SPIRES].

[38] P.B. Arnold, *Hot B violation, the lattice and hard thermal loops*, *Phys. Rev.* **D 55** (1997) 7781 [hep-ph/9701393] [SPIRES].

[39] The MILC collaboration, A. Bazavov et al., *Results from the MILC collaboration's* SU*(3) chiral perturbation theory analysis*, PoS(LAT2009)079 [arXiv:0910.3618] [SPIRES].

[40] S.Y. Khlebnikov and M.E. Shaposhnikov, *The Statistical Theory of Anomalous Fermion Number Nonconservation*, *Nucl. Phys.* **B 308** (1988) 885 [SPIRES].

[41] D.T. Son and A.O. Starinets, *Minkowski-space correlators in AdS/CFT correspondence: Recipe and applications*, *JHEP* **09** (2002) 042 [hep-th/0205051] [SPIRES].

[42] H.B. Meyer, *Transport properties of the quark-gluon plasma from lattice QCD*, *Nucl. Phys.* **A 830** (2009) 641c [arXiv:0907.4095] [SPIRES].

[43] G.D. Moore, *Motion of Chern-Simons Number at High Temperatures under a Chemical Potential*, *Nucl. Phys.* **B 480** (1996) 657 [hep-ph/9603384] [SPIRES].

[44] M. Lüscher, *Topology of Lattice Gauge Fields*, *Commun. Math. Phys.* **85** (1982) 39 [SPIRES].

[45] P. Woit, *Topological Charge in Lattice Gauge Theory*, *Phys. Rev. Lett.* **51** (1983) 638 [SPIRES].

[46] P. Woit, *Topology and Lattice Gauge Fields*, *Nucl. Phys.* **B 262** (1985) 284 [SPIRES].

[47] A. Phillips and D. Stone, *Lattice Gauge Fields, Principal Bundles and the Calculation of Topological Charge*, *Commun. Math. Phys.* **103** (1986) 599 [SPIRES].

[48] D.Y. Grigoriev, V.A. Rubakov and M.E. Shaposhnikov, *Sphaleron Transitions at Finite Temperatures: Numerical Study in (1+1)-Dimensions*, *Phys. Lett.* **B 216** (1989) 172 [SPIRES].

[49] D. Bödeker, *Classical real time correlation functions and quantum corrections at finite temperature*, *Nucl. Phys.* **B 486** (1997) 500 [hep-th/9609170] [SPIRES].

[50] E. Braaten and R.D. Pisarski, *Soft Amplitudes in Hot Gauge Theories: A General Analysis*, *Nucl. Phys.* **B 337** (1990) 569 [SPIRES].

JHEP02(2011)105

[51] J. Frenkel and J.C. Taylor, *High Temperature Limit of Thermal QCD*, *Nucl. Phys.* **B 334** (1990) 199 [SPIRES].

[52] G.D. Moore, *Measuring the broken phase sphaleron rate nonperturbatively*, *Phys. Rev.* **D 59** (1999) 014503 [hep-ph/9805264] [SPIRES].

[53] G.D. Moore, *O(a) errors in* $3-D$ SU*(N) Higgs theories*, *Nucl. Phys.* **B 523** (1998) 569 [hep-lat/9709053] [SPIRES].

[54] M. Laine, G.D. Moore, O. Philipsen and M. Tassler, *Heavy Quark Thermalization in Classical Lattice Gauge Theory: Lessons for Strongly-Coupled QCD*, *JHEP* **05** (2009) 014 [arXiv:0902.2856] [SPIRES].

JHEP02(2011)105